Characterization of atmospheric ammonia near Fort Worth, TX – Part I. Dynamics of gaseous ammonia

L. Gong[1], R. Lewicki[2,3], R. J. Griffin[1], B. Karakurt Cevik[1], A. P. Rutter[1,4], F. K. Tittel[2], J. H. Flynn[5], B. L. Lefer[5], E. Scheuer[6], J. E. Dibb[6], and S. Kim[7,8]

[1]Department of Civil and Environmental Engineering, Rice University, Houston, TX, USA

[2]Department of Electrical and Computer Engineering, Rice University, Houston, TX, USA

[3]Now at Sentinel Photonics, Monmouth Junction, NJ, USA

[4]Now at Sonoma Technology, Inc. Petaluma, CA, USA

[5]Department of Earth and Atmospheric Sciences, University of Houston, Houston, TX, USA

[6]Institute for the Study of Earth, Oceans, and Space, University of New Hampshire, Durham, NH, USA

[7]Earth and Sun Systems Laboratory, Atmospheric Chemistry Division, National Center for Atmospheric Research, Boulder, CO, USA

[8]Now at Department of Earth System Science, University of California, Irvine, CA, USA

Correspondence to: R. J. Griffin (rob.griffin@rice.edu)

Abstract

The present work reports the experimental results from the first field investigation of atmospheric ammonia (NH_3) in the Fort Worth, TX area. The NH_3 measurements were conducted in the early summer of 2011 (30 May – 30 June) using a 10.4-μm external cavity quantum cascade laser-based sensor employing conventional photo-acoustic spectroscopy; supplementary data for other gaseous species were collected simultaneously. NH_3 mixing ratios showed a large amount of variability, ranging from 0.35 to 10.07 ppb, with a mean of 2.68 ± 1.59 (1σ) ppb. The diurnal profile of NH_3 exhibited a daytime increase, likely due to increasing temperatures affecting temperature-dependent sources in the study region. A large church near the sampling location caused unusual traffic patterns. Automobiles might be potential sources of NH_3 on Sundays according to the Pearson's correlation coefficient between NH_3 and carbon monoxide, but the relationship did not exist on weekdays and Saturdays, probably due to decreased traffic volume and different traffic composition. Daytime-nighttime comparisons suggest insignificant changes in the correlation coefficients between NH_3 and other air pollutants. According to the results from the EPA PMF 3.0 model, biogenic (primarily vegetation and soil) emissions were major contributors to gas-phase NH_3 levels measured at the suburban site during the campaign. In addition, agriculture (especially livestock-related activities) also was expected to be a potentially significant source of NH_3 based on the nature of the region. The dynamic behavior of NH_3 highlights its importance in atmospheric chemistry and indicates its potential effects on the local and regional air quality.

Keywords: ammonia, air quality, Pearson's correlation, source attribution.

1. Introduction

As a primary basic trace gas, ammonia (NH_3) plays a significant role in atmospheric chemistry. It is emitted into the atmosphere from a variety of sources, and the ambient mixing ratios of NH_3 usually vary between 0.1 and 10 parts per billion (ppb), depending on the proximity to the source [*Seinfeld and Pandis*, 2006]. In the past decade, there have been increasing concerns about atmospheric NH_3 due to its impact on the formation of particulate matter (PM), also known as atmospheric aerosol. NH_3 can lead to the production of ammonium salts such as $(NH_4)_2SO_4$, NH_4NO_3, and NH_4Cl through chemical reactions with sulfuric, nitric, and hydrochloric acids, respectively. These secondary aerosols have strong implications for a series of environmental issues (e.g., atmospheric visibility and nutrient cycling). In addition, they can alter the Earth's energy flow via direct effects, and influence the cloud albedo and lifetime via indirect effects. The largest uncertainties among all radiative forcing components in global climate models are associated with PM [*IPCC*, 2007]. Enhanced levels of PM also have been linked statistically to increased rates of morbidity and mortality among the exposed populations [*Dockery*, 2001; *MacNee and Donaldson*, 2003].

Previous measurements of atmospheric NH_3 were conducted mainly near source areas (e.g., concentrated animal feeding operations, croplands, and forests) [*Barthelmie and Pryor*, 1998; *Lefer et al*., 1999; *Pryor et al*., 2001; *Bajwa et al*., 2006; *Wilson and Serre*, 2007; *Todd et al*., 2008]. Recently, researchers have paid more attention to NH_3 studies at urban sampling locations where relative contributions from industrial processes and traffic emissions are more significant [*Ianniello et al*., 2010; *Gong et al*., 2011; *Meng et al*., 2011; *Pandolfi et al*., 2012]. Many techniques have been developed and utilized for NH_3

measurements including wet chemistry, laser absorption spectroscopy, cavity ring down spectroscopy, chemical ionization mass spectrometry, ion mobility spectrometry, and fourier transform infrared spectroscopy [*von Bobrutzki et al*., 2010]. *Schwab et al*. [2007] pointed out that the instrument response time, as a critical parameter in environmental measurements, was sensitive to sample handing materials and varied among different methods, which posed substantial difficulties for inter-comparison. Photo-acoustic spectroscopy (PAS) used in this study enables the direct measurement of atmospheric NH_3, improves the temporal resolution and detection limit, and eliminates the interference from particulate ammonium.

The Toxics Release Inventory (TRI) of the United States Environmental Protection Agency (U.S. EPA) highlights the importance of NH_3 as an air pollutant in urban communities nationwide [*U.S. EPA*, 2010]. Figure 1 (a) presents the total air releases (2.4 million pounds) by species in the Dallas-Fort Worth (DFW) metropolitan area according to the TRI in 2010 [*U.S. EPA*, 2010]. It can be seen that NH_3 has the largest individual magnitude of emissions compared to other air wastes. According to the U.S. EPA National Emissions Inventory (NEI), agricultural and automobile activities are major contributors to gaseous NH_3 emissions. Figure 1 (b) summarizes the NEI NH_3 emissions (642.6 million pounds) by source categories specifically for all of Texas in 2008 and indicates that livestock waste and fertilizer application account for approximately 90% of the annual NH_3 emissions [*U.S. EPA*, 2008]. In addition, *Corsi et al*. [2000] reported the first estimation of non-point source NH_3 emissions in Texas. Measurements of NH_3 emissions from pine and oak forests further improved the non-industrial NH_3 emissions inventory in Texas [*Corsi et al*., 2002; *Sarwar, et al*., 2005].

Despite the emissions information described above, there is limited information about measured atmospheric NH_3 levels in Texas. Recently, *Nowak et al*. [2010] and *Gong et al*. [2011, 2013a] characterized gas-phase NH_3 in Greater Houston, suggesting that the heavily industrialized Houston Ship Channel is a major NH_3 hotspot and indicating the impact that NH_3 can have on atmospheric particle number and mass concentrations. However, observational data regarding NH_3 concentrations in the DFW area currently are very scarce in the published literature. This particular region, with a population of 6.4 million people, has experienced rapid economic growth. Nevertheless, air pollution problems threaten sustainable development [*Grodach*, 2011]. Therefore, relevant field investigations of the dynamics of gaseous NH_3 in the DFW area are highly valuable and provide new insights into local and regional air quality, especially the impact of NH_3 on PM formation which is described in Part II [*Gong et al*., 2013b].

2. Experimental Methods

2.1 Instrumentation

In this study, atmospheric NH_3 measurements were performed using a 10.4-μm external cavity quantum cascade laser (EC-QCL) based-sensor employing conventional PAS previously described in more detail [*Gong et al*., 2011]. This state-of-the-art optical technique achieves a detection limit of 0.7 ppb with a response time of seconds and an accuracy of ±7%. The high sensitivity and selectivity allows effective capture of the fast-changing behaviors of NH_3. The sensor box and inlet were heated to ~38 ^{o}C, and a 1.7 m length of 13 mm (outside diameter) PTFE Teflon® tubing was used as the sampling line to

minimize NH_3 adsorption. NH_3 data below the detection limit were substituted with one half of the detection limit in the data analysis in the following sections [*U.S. EPA*, 2008]. Auxiliary data of other important trace gases (e.g., carbon monoxide (CO), sulfur dioxide (SO_2), nitrogen oxides (NO_x), total reactive nitrogen species (NO_y), nitric acid (HNO_3), soluble chloride (presumably hydrochloric acid (HCl)), and volatile organic compounds (VOCs)) also were collected simultaneously. Detailed information about measurement techniques can be found in Table 1.

2.2 Site Description

A one-month campaign was conducted at the Eagle Mountain Lake continuous ambient monitoring station (CAMS 75) operated by the Texas Commission on Environmental Quality (TCEQ) at 32°59'16"N and 97°28'37"W in Tarrant County. It is ~17 miles northwest of downtown Fort Worth and ~42 miles northwest of downtown Dallas. The CAMS is equipped with an automated gas chromatograph, ozone (O_3) and NO_x analyzers, and meteorological instrumentation. Real-time monitoring has been active since 6 June 2000. The Texas National Guard manages the land, which is flat, has an elevation of 226 m above sea level, and is surrounded by shrubs, grasses, and trees.

NH_3 was measured as a complement to a summer project that focused primarily on the examination of O_3 formation mechanisms in the DFW area. All instruments except the mist chamber-ion chromatography system were deployed in a climate-controlled trailer at ground level. The NH_3 sensor had an inlet height of ~2.5 m above the surface. This site is

expected to be influenced by urban (e.g., regional transport from the city center), industrial (e.g., natural gas operations), and biogenic (e.g., vegetation) sources. The U.S. Department of Agriculture (USDA) Texas livestock inventory estimated 15,000 cattle in Tarrant County in 2011, and 57.8% of county land was classified as pasture in the 2007 Census of Agriculture [*USDA*, 2007, 2011]. Cows sometimes were observed near the site during the measurements. Figure 2 shows the sampling location as well as the nearby point sources of NH_3 specified in the U.S. EPA's NEI and TRI, which include food manufacturing, chemical production, and an electricity station.

3. Results and Discussion

3.1 NH_3 Mixing Ratio Profile

A time series of hourly-averaged NH_3 data over the entire campaign (30 May 2011 – 30 June 2011) is given in Figure 3. The gaps in the time series indicate sensor calibration and system resetting. The mixing ratios of NH_3 showed a large amount of variability, ranging from 0.35 to 10.07 ppb with a mean of 2.68 ± 1.59 (1σ) ppb, comparable to the results observed at some other suburban sites [*Ellis et al*., 2011]. The statistics of the datasets for NH_3 as well as other measured gaseous species are listed in Table 2. Since no comparison can be made at this time due to the lack of NH_3 information in the DFW area in the literature, long-term continuous NH_3 monitoring in the future is necessary to explore inter-annual variation and seasonality of NH_3. The prominent variability on the hourly time scale also emphasizes the significance of the use of high time-resolution instruments to

measure NH_3, which is considerably affected by physical and chemical processes in the atmosphere.

Moreover, NH_3 levels were relatively larger during the first week (4.35 ± 2.13 ppb) compared to other periods of the measurements (2.31 ± 1.32 ppb). This phenomenon was probably related to weaker air movement resulting from lower wind speed. Similarly, relatively higher levels of CO (173.04 ± 48.65 ppb) and NO_x (5.46 ± 5.91 ppb) were observed during the first week compared to other periods of the measurements (125.67 ± 32.33 ppb and 2.95 ± 3.18 ppb, respectively), suggesting that stronger local fuel combustion sources might have influenced the site and contributed to the elevated mixing ratios of these air pollutants during the first week. Further discussion can be found in Section 3.4.

3.2 Diurnal Variation

Figure 4 presents the diurnal profiles of NH_3 mixing ratios and ambient temperatures (the bottom whisker, box bottom, line inside the box, box top, and top whisker represent the 10th, 25th, 50th, 75th, and 90th percentiles of the data, and the continuous solid lines represent mean values, respectively). In general, NH_3 increased in the morning starting from 05:00 CST and peaked in the early afternoon between 14:00-15:00 CST, after which the levels decreased and remained relatively low during nighttime, presumably due to the decrease of sources. The daytime behavior of NH_3 was likely associated with increasing temperatures (30.2 ± 4.2 ^{o}C) affecting temperature-dependent sources such as volatilization

of animal waste and vegetation/soil through photosynthetic processes [*Krupa*, 2003; *Mukhtar et al*., 2009; *Bash et al*., 2010; *Riddick et al*., 2012].

The dynamics of LIDAR-measured planetary boundary layer (PBL) heights were consistent from day to day over the entire campaign. The height remained low (~500 m) during nighttime and the PBL did not break up until 07:00 CST, while NH_3 mixing ratios began to increase at 05:00 CST. Therefore, downward vertical mixing of NH_3 from the residual layer is ruled out as a contributing source of NH_3 in the morning.

Figure 5 summarizes the hourly-averaged data for NH_3, CO, SO_2, NO_x, HNO_3, and HCl, displaying distinctive characteristics and dynamics among species. As good indicators of vehicular emissions, CO and NO_x had similar trends, with levels that increased in the early morning (04:00-05:00 CST), reached maximum values at 06:00 CST, and dropped quickly and dramatically until second peaks occurred in the late afternoon (18:00-21:00 CST). The increases were a result of enhanced traffic volume during rush hour together with the lingering effect of a shallow nocturnal boundary layer (morning) or a developing nocturnal boundary layer (evening). However, none of these spikes were exactly coincident with temporal patterns of NH_3. Motor vehicles were unlikely to have been major sources of NH_3 during the measurement periods, despite the fact that three-way catalytic converters have been found to be significant producers of NH_3 [*Shelef and McCabe*, 2000; *Heck and Farrauto*, 2001; *Kašpar et al*., 2003; *Heeb et al*., 2006]. In the rural/suburban area of the present study, heavy-duty diesel trucks, which have minor contributions to NH_3 but emit tremendous amounts of NO_x, account for a large fraction of traffic composition, as opposed to light-duty gasoline cars, which have the largest emission factors of NH_3 among all on-road

vehicles [*Harley*, 2009; *Kean et al*., 2009]. This is a likely explanation for these observations. Additionally, a cargo/freight rail near the site was not considered as a NH_3 source according to the NEI.

Sulfur dioxide mixing ratios did not change significantly during the daytime, but they became elevated at night, indicating that PBL dynamics played a vital role. Based on this profile, SO_2 likely was emitted from sources different than those of NH_3.

The changes in HNO_3 and HCl levels tracked one another closely. For both acidic trace gases, morning enhancements and mid-day peaks were observed. Nitric acid is primarily formed by oxidation of NO_x in the atmosphere, and strong solar radiation facilitates photochemical processes. In this work, total photosynthetically available radiation (W m^{-2}) reached maximum values at 12:00 CST. Hydrochloric acid is mainly produced by biomass burning/coal combustion and the salt metathesis reaction between HNO_3 and sodium chloride. In addition, NH_3 was more abundant than HNO_3 and HCl. The average ratio of NH_3 to the summation of HNO_3 and HCl (calculated in units of μmol m^{-3}) during the measurements was 4.13 ± 4.02. Larger ratios (>10) sometimes were observed when higher NH_3 levels and significantly lower HNO_3 and HCl levels were present in the early morning (06:00-07:00 CST) as shown in Figure 6. Some removal mechanisms and/or processes other than gas-phase chemistry may govern the concentration levels of these acidic gases.

Remarkable differences in behavior exist between rural/suburban- and urban-scale NH_3 measurements. For example, at a near-downtown Houston site, *Gong et al.* [2011] observed a sharp decrease in NH_3 around mid-day when the ratio of NO_x to NO_y, as an indicator of the photochemical age of air masses or plumes, also reached the minimum value.

By contrast, no such phenomenon occurred in the present work in which NH_3 mixing ratios continuously increased through the early afternoon (14:00-15:00 CST). Although HNO_3 and HCl peaked at mid-day, increased emissions from temperature-dependent sources under the most intense sunlight at noon might significantly replenish NH_3 and overweigh any loss mechanisms.

3.3 Weekday-Weekend and Daytime-Nighttime Behaviors

As will be shown in the next section, the winds uniformly emanated from the southeast sector throughout the campaign, offering little variability in source regions. In this section we consider variability arising from weekday-weekend and daytime-nighttime differences. In order to further investigate NH_3 behavior, the datasets were divided into weekday/weekend and daytime/nighttime. Here, daytime and nighttime are consistently defined as periods of 06:00-19:00 CST and 19:00-06:00 CST, respectively. Table 3 summarizes the Pearson's correlation coefficients between NH_3 and other traces gases during different time periods. The coefficient between NH_3 and CO was significantly larger on Sundays (0.62) than weekdays (0.09) and Saturdays (0.11), but there was no statistically meaningful difference between daytime and nighttime. There was a significant increase in traffic volume due to human activities on Sundays because of a large church very close to the site. It is known that gasoline engines emit ~10 times more CO compared to diesel engines [*Fairbanks*, 1997]. Also as discussed above, gasoline-powered cars have much larger emission rates of NH_3 than other vehicles. The combined effects were likely responsible for

the observation, suggesting that automobiles might be contributing NH_3 on Sundays when the maximal mixing ratio of CO also occurred.

The weak relationships between NH_3 and SO_2 were consistent during all periods, while the correlation coefficients between NH_3 and NO_x, NO_y, NO_z (=NO_y-NO_x), and HNO_3 displayed a similar trend for that of NH_3 versus CO, indicating stronger relationships on Sundays. This is probably due to the co-emission of NH_3 and NO_x from motor vehicles and subsequent rapid oxidation of NO_x via rapid photochemical processes. The relationship between NH_3 and HCl was slightly stronger on weekdays than weekends, though the reason for this remains unclear. HNO_3 and HCl have similar diurnal variations as shown in Figure 5, but the correlation coefficient between two species is only 0.09 using the entire dataset. It is also noted that the good relationship between HNO_3 and HCl was observed within nearly any given day, but it is not the case after combining several different days. The contribution from different source regions was eliminated as a plausible reason for this phenomenon because the wind direction was relatively consistent during the measurement period. The algorithm used in the regression analysis can not solve the HNO_3-HCl puzzle and can not explain the large discrepancy between NH_3-HNO_3 and NH_3-HCl correlations.

3.4 Source Attribution

During the one-month campaign, the wind mainly blew from the southeast sector at the site, illustrated by Figure 7. Because of this relative consistency, almost no information about the dependence of NH_3 on wind direction can be drawn. There are six specific point

sources of NH_3 in the study region listed in the NEI and TRI. Most of the time, the site was downwind of these sources. As shown in Figure 2, they are in the range of ~13 to ~22 miles southeast of the site. Given an average wind speed of 12 miles per hour, emissions events at those facilities could possibly affect measured NH_3 mixing ratios at the site within one to two hours.

Besides industry, agriculture, especially livestock-related activities, is an additional potential contributor to NH_3. A review paper reported average emission factors of NH_3 for dairy farms (59 g milk cow^{-1} day^{-1}) and beef feedlots (119 g beef cow^{-1} day^{-1}) using data from forty relevant studies in North America and Europe [*Hristov et al*., 2011]. Based on the cattle population in Tarrant County, the estimated emissions of NH_3 from cows are about 1.3 tons day^{-1}. However, the tracks from animals (not only cattle but also deer and other wildlife) near the site could not be documented. Hence, it is hard to pinpoint the accurate source location and to evaluate quantitatively these effects with respect to observed values.

Natural emissions of NH_3 from vegetation and soil have been found to be important, and they often increase as ambient temperatures increase [*Robarge et al*., 2002; *Sutton et al*., 2009]. Forests emit NH_3 more strongly than grassland and shrub land [*Battye et al*., 2003]. Simultaneous measurements of NH_3 fluxes in the future are desirable to better understand the NH_3 exchange between plants, soil, and atmosphere, and to better quantify the related contributions from biogenic sources. Based on the emission factors in the literature and geographic/geological information in Tarrant County, the estimated emissions of NH_3 from soils and vegetation are about 0.15 ton day^{-1} [*TPWD*, 1984; *BEG*, 2000; *Battye et al*., 2003].

Air masses rarely were transported from the south-southwest (occurrence frequency = 2.3%) and passed over Eagle Mountain Lake (~0.5 mile from the site). It is known that NH_3 has a relatively large Henry's law constant. Thus, the occasional plumes coming in that direction over the water body probably had a very small impact on NH_3 levels. There are likely less animals (especially cows) and vegetation along the lake area than in the pastures close to the site. In addition, fewer industrial activities in the southwest region might contribute to relatively lower NH_3 levels. Specifically, the mean NH_3 mixing ratio was 2.0 ppb (a decrease of ~26% compared to the campaign-average value of 2.7 ppb) when the wind blew from that sector.

The EPA Positive Matrix Factorization (PMF) 3.0 model was used to conduct source attribution in which NH_3 and ancillary data for other gaseous species (e.g., VOCs including ~40 compounds) were employed as inputs [*Paatero and Tapper*, 1994; *Paatero*, 1997]. In addition to a concentration file, an uncertainty file associated with the collected samples/data was used, which can be derived based on the user guide. PMF requires the user to have a general understanding of the dataset (e.g., potential sources influencing the study region) and to choose the number of source categories or factors. It also allows the user to examine the initial assumption for factors according to the base run results and make the relevant model reconstruction if needed. In this work, a four-factor solution was found including biogenic (isoprene/monoterpene), natural gas/industry (ethane/ethylene/propane/propylene), heavy duty motor vehicles (*n*-decane), and light duty motor vehicles (*o*-xylene/toluene). These were identified using dominant or key species accordingly while other measured trace gases and VOCs were also fed into the model. The simulation results explicitly show that

biogenic (74.1%) is the largest source category of NH_3, followed by light duty vehicles (12.1%), natural gas/industry (9.4%), and heavy duty vehicles (4.4%). As unique chemical signatures of biogenic emissions, isoprene and monoterpene as well as the non-indicator, NH_3, were predominantly apportioned to this particular factor resolved by PMF. The preliminary analysis for biogenic sector implies that livestock might account for approximately 66.4% of total NH_3 emissions in the present study assuming that biogenic source category mainly consists of soil, plants, and animals (especially cows). This upper bound estimate is calculated by multiplying the entire contribution from the biogenic source category (74.1%) by the estimate proportion of cows in biogenic emissions derived from previously estimated emission rates of cows (1.3 tons day^{-1}) and soils and vegetation (0.15 tons day^{-1}). Future work with updated species categorization and additional exploration of sources in the area is needed to improve the constraints in the model. In addition, long-term datasets are required in PMF to investigate the aggregate contributions (e.g., yearly and seasonal contributions) from different factors.

PMF also was used to examine the observation of higher NH_3 levels during the first week of the campaign. The simulation results clearly show that the relative contributions from industry increase from 9.4% to 18.9% using the dataset only covering that period. This prominent change is likely due to the enhanced tracers of industry. For example, elevated levels of ethane (9.48 ± 9.22 ppb), ethylene (0.27 ± 0.21 ppb), propane (3.47 ± 3.40 ppb), and propylene (0.15 ± 0.09 ppb) were measured during the first week compared to other periods of the measurements (4.76 ± 4.32 ppb, 0.15 ± 0.09 ppb, 1.96 ± 1.75 ppb, and 0.09 ± 0.04 ppb, respectively). It suggests that local industrial activities have potentially

significant influences on atmospheric NH_3 mixing ratios in the study region. Improved NH_3 emission inventories with better documentation and monitoring of anthropogenic sources (especially industry) are also needed.

4. Conclusions

Atmospheric NH_3 measurements were made northwest of Fort Worth in the early summer of 2011 (30 May – 30 June) using a 10.4-μm EC-QCL-based sensor employing conventional PAS. Ammonia mixing ratios showed a large amount of variability, ranging from 0.35 to 10.07 ppb with a mean of 2.68 ± 1.59 ppb. A daytime increase was observed in the diurnal profile of NH_3, likely due to increasing temperatures affecting temperature-dependent sources (e.g., volatilization of animal waste and vegetation). A moderate correlation ($r = 0.62$) between NH_3 and CO was found on Sundays, indicating that motor vehicles might be potential sources of NH_3 during those periods, but there was no relationship on weekdays and Saturdays as a consequence of lower traffic volume and different traffic composition. The correlation coefficients between NH_3 and other air pollutants did not change significantly during daytime versus nighttime. Biogenic and agricultural emissions appear to be major contributors to gaseous NH_3 levels measured at the suburban site in this study. However, detailed source identification was impeded by many factors, such as the lack of relevant NH_3 data in the literature and the paucity of sufficient emission inventory data. Extended measurements in the future are needed to fully examine the seasonality of NH_3 and to further investigate the influence of local and regional sources on NH_3 levels in the DFW area.

Acknowledgements

This study was supported by the Mid-InfraRed Technologies for Health and the Environment (MIRTHE) Center and National Science Foundation (NSF) under grant No. EEC-0540832 and the TCEQ Air Quality Research Program. The authors gratefully acknowledge the U.S. EPA for supplying the PMF 3.0 model (http://www.epa.gov/heasd/products/pmf/pmf.html). The authors also would like to thank Melanie Calzada, Caroline Gutierrez, and Kabindra Shakya for their help in data collection in the field and the Texas National Guard for providing access to the Eagle Mountain Lake site.

Reference

Bajwa, K. S., V. P. Aneja, and S. P. Arya (2006), Measurement and estimation of ammonia emissions from lagoon-atmosphere interface using a coupled mass transfer and chemical reactions model, and an equilibrium model, *Atmos. Environ., 40*, 275-286.

Barthelmie, R. J., and S. C. Pryor (1998), Implications of ammonia emissions for fine aerosol formation and visibility impairment: a case study from the lower Fraser Valley, British Columbia, *Atmos. Environ., 32*, 345-352.

Bash, J. O., J. T. Walker, G. G. Katul, M. R. Jones, E. Nemitz, and W. P. Robarg (2010), Estimation of in-canopy ammonia sources and sinks in a fertilized *Zea mays* field, *Environ. Sci. Technol., 44*, 1683-1689.

Battye, W., V. P. Aneja, and P. A. Roelle (2003), Evaluation and improvement of ammonia emissions inventories, *Atmos. Environ., 37*, 3873-3883.

Bureau of Economic Geology, The University of Texas at Austin (2000), Vegetation/cover types of Texas 2000.

Corsi, R. L., V. M. Torres, G. Carter, K. Dombowski, M. Dondelle, S. Fredenberg, S. Takahama, and T. Taylor (2000), Nonpoint source ammonia emissions in Texas: a first estimate, *prepared for the Texas Natural Resource Conservation Commission, Austin, TX*.

Corsi, R., J. Banks, K. Kinney, and M. G. Sarwar (2002), Non-point source ammonia emissions in Texas: estimation methods, pitfalls, corrections, and comparisons, *prepared for the Texas Natural Resource Conservation Commission, Austin, TX*.

Dockery, D. W. (2001), Epidemiologic evidence of cardiovascular effects of particulate air pollution, *Environ. Health Persp., 109*, 483-486.

Ellis, R. A., J. G. Murphy, M. Z. Markovic, T. C. VandenBoer, P. A. Makar, J. Brook, and C. Mihele (2011), The influence of gas-particle partitioning and surface-atmosphere exchange

on ammonia during BAQS-Met, *Atmos. Chem. Phys., 11,* 133-145, doi:10.5194/acp-11-133-2011.

Fairbanks, J. W. (1997), Diesel engines vs. spark ignition gasoline engines – which is greener?, *Proceedings of the 1997 Diesel Engine Emissions Reduction Workshop*, La Jolla, California. July 28-31. Washington, DC: DOE.

Gong, L., R. Lewicki, R. J. Griffin, J. H. Flynn, B. L. Lefer, and F. K. Tittel (2011), Atmospheric ammonia measurements in Houston, TX using an external-cavity quantum cascade laser-based sensor, *Atmos. Chem. Phys., 11*, 9721–9733, doi:10.5194/acp-11-9721-2011.

Gong, L., R. Lewicki, R. J. Griffin, F. K. Tittel, C. R. Lonsdale, R. G. Stevens, J. R. Pierce, Q. G. J. Malloy, S. A. Travis, L. M. Bobmanuel, B. L. Lefer, and J. H. Flynn (2013a), Role of atmospheric ammonia in particulate matter formation in Houston during summertime, *Atmos. Environ.*, in press.

Gong, L., R. Lewicki, B. Karakurt Cevik, A. P. Rutter, R. J. Griffin, F. K. Tittel, J. H. Flynn, B. L. Lefer, E. Scheuer, J. E. Dibb, and S. Kim (2013b), Characterization of atmospheric ammonia near Fort Worth, TX – Part II. Impact of ammonia on particulate matter formation, submitted to *J. Geophys. Res.*

Grodach, C. (2011), Barriers to sustainable economic development: The Dallas-Fort Worth experience, *Cities, 28*, 300-309.

Harley, R. (2009), On-road measurement of light-duty gasoline and heavy-duty diesel vehicle emissions, *California Air Resources Board Research Final Report.*

Heck, R. M., and R. J. Farrauto (2001), Automobile exhaust catalysts, *Appl. Catal. A: General, 221*, 443-457.

Heeb, N. V., A. Forss, S. Brühlmann, R. Lüscher, C. J. Saxer, and P. Hug (2006), Three-way catalyst-induced formation of ammonia—velocity- and acceleration-dependent emission factors, *Atmos. Environ., 40*, 5986-5997.

Hristov, A. N., M. Hanigan, A. Cole, R. Todd, T. A. McAllister, P. M. Ndegwa, and A. Rotz (2011), Review: Ammonia emissions from dairy farms and beef feedlots, *Can. J. Anim. Sci*., *91*, 1-35.

Ianniello, A., F. Spataro, G. Esposito, I. Allegrini, E. Rantica, M. P. Ancora, M. Hu, and T. Zhu (2010), Occurrence of gas phase ammonia in the area of Beijing (China), *Atmos. Chem. Phys., 10*, 9487–9503, doi:10.5194/acp-10-9487-2010.

IPCC (2007), Climate Change 2007. Synthesis Report. Contribution of Working Groups I, II and III to the Fourth Assessment Report of the Intergovernmental Panel on Climate Change [Core Writing Team, Pachauri, R. K. and Reisinger, A. (eds.)]. *IPCC*, Geneva, Switzerland, 104 pp.

Kašpar, J., P. Fornasiero, and N. Hickey (2003), Automotive catalytic converters: current status and some perspectives, *Catal. Today*, 77, 419-449.

Kean, A. J., D. Littlejohn, G. A. Ban-Weiss, R. A. Harley, T. W. Kirchstetter, and M. M. Lunden (2009), Trends in on-road vehicle emissions of ammonia, *Atmos. Environ., 43*, 1565-1570.

Krupa, S. V. (2003), Effects of atmospheric ammonia (NH_3) on terrestrial vegetation: a review, *Environ. Pollut., 124*, 179-221.

Lefer, B. L., R. W. Talbot, and J. W. Munger (1999), Nitric acid and ammonia at a rural

northeastern U.S. site, *J. Geophys. Res., 115(D1)*, doi:10.1029/1998JD100016.
MacNee, W., and K. Donaldson (2003), Mechanism of lung injury caused by PM_{10} and ultrafine particles with special reference to COPD, *Eur. Respir. J., 21*, Suppl. 40, 47s-51s.
Meng, Z. Y., W. L. Lin, X. M. Jiang, P. Yan, Y. Wang, Y. M. Zhang, X. F. Jia, and X. L. Yu (2011), Characteristics of atmospheric ammonia over Beijing, China, *Atmos. Chem. Phys.*, *11*, 6139–6151, doi:10.5194/acp-11-6139-2011.
Mukhtar, S., A. Mutlu, R. E. Lacey, and C. B. Parnell (2009), Seasonal ammonia emissions from a free-stall dairy in central Texas, *J. Air Waste Manage. Assoc., 69*, 613-618.
Nowak, J. B., J. A. Neuman, R. Bahreini, C. A. Brock, A. M. Middlebrook, A. G. Wollny, J. S. Holloway, J. Peischl, T. B. Ryerson, and F. C. Fehsenfeld (2010), Airborne observations of ammonia and ammonium nitrate formation over Houston, Texas, *J. Geophys. Res., 115*, D22304, doi:10.1029/2010JD014195.
Paatero, P., and U. Tapper (1994), Positive matrix factorization: a non-negative factor model with optimal utilization of error estimates of data values, *Environmetrics, 5*, 111-126.
Paatero, P. (1997), Least squares formulation of robust non-negative factor analysis, *Chemometr. Intell. Lab. Syst., 37*, 23-35.
Pandolfi, M., F. Amato, C. Reche, A. Alastuey, R. P. Otjes, M. J. Blom, and X. Querol (2012), Summer ammonia measurements in a densely populated Mediterranean city, *Atmos. Chem. Phys.*, 12, 7557-7575.
Pryor, S. C., R. J. Barthelmie, L. L. Sørensen, and B. Jensen (2001), Ammonia concentrations and fluxes over a forest in the midwestern USA, *Atmos. Environ., 35*, 5634-5656.
Riddick, S. N., U. Dragosits, T. D. Blackall, F. Daunt, S. Wanless, and M. A. Sutton (2012), The global distribution of ammonia emissions from seabird colonies, *Atmos. Environ., 55*, 319-327.
Robarge, W. P., J. T. Walker, R. B. McCulloch, and G. Murray (2002), Atmospheric concentrations of ammonia and ammonium at an agricultural site in the southeast United States, *Atmos. Environ., 36*, 1661-1674, 2002.
Sarwar, G., R. L. Corsi, K. A. Kinney, J. A. Banks, V. M. Torres, and C. Schmidt (2005), Measurements of ammonia emissions from oak and pine forests and development of a non-industrial ammonia emissions inventory in Texas, *Atmos. Environ., 39*, 7137-7153.
Schwab, J. J., Y. Li, M. S. Bae, K. L. Demerjian, J. Hou, X. Zhou, B. Jensen, and S. C. Pryor (2007), A laboratory intercomparison of real-time gaseous ammonia measurement methods, *Environ. Sci. Technol., 41*, 8412-8419.
Seinfeld, J. H., and S. N. Pandis (2006), Atmospheric Chemistry and Physics: From Air Pollution to Climate Change, *John Wiley*, New York.
Shelef, M., and R. W. McCabe (2000), Twenty-five years after introduction of automotive catalysts: what next?, *Catal. Today, 62*, 35-50.
Sutton, M., S. Reis, and S. Baker (2009), Atmospheric ammonia: detecting emission changes and environmental impacts. Results of an expert workshop under the convention on long-range transboundary air pollution, *Springer Publishing*, New York.
Texas Parks & Wildlife Department (1984), The Vegetation types of Texas, http://www.tpwd.state.tx.us/publications/pwdpubs/pwd_bn_w7000_0120
Todd, R. W., N. A. Cole, R. N. Clark, T. K. Flesch, L. A. Harper, and B. H. Baek (2008), Ammonia emissions from a beef cattle feedyard on the southern High Plains, *Atmos.*

Environ., 42, 6797-6805.
USDA National Agriculture Statistics Service (2007), 2007 Census of Agriculture, http://www.agcensus.usda.gov/Publications/2007/Full_Report/Census_by_State/Texas/
USDA National Agriculture Statistics Service (2011), Texas Livestock Inventory, http://www.nass.usda.gov/Statistics_by_State/Texas/index.asp
U.S. EPA (2008), EPA Positive Matrix Factorization (PMF) 3.0 Fundamentals & User Guide, http://www.epa.gov/heasd/documents/EPA PMF 3.0 User Guide v16_092208_final.pdf.
U.S. EPA (2008), National Emissions Inventory (NEI) Data Version 2, http://www.epa.gov/ttn/chief/net/2008inventory.html.
U.S. EPA (2010), Toxics Release Inventory (TRI) National Analysis, http://www.epa.gov/tri/tridata/tri10/nationalanalysis/index.htm.
von Bobrutzki, K., C. F. Braban, D. Famulari, S. K. Jones, T. Blackall, T. E. L. Smith, M. Blom, H. Coe, M. Gallagher, M. Ghalaieny, M. R. McGillen, C. J. Percival, J. D. Whitehead, R. Ellis, J. Murphy, A. Mohacsi, A. Pogany, H. Junninen, S. Rantanen, M. A. Sutton, and E. Nemitz (2010), Field inter-comparison of eleven atmospheric ammonia measurement techniques, *Atmos. Meas. Tech., 3,* 91-112, doi:10.5194/amt-3-91-2010.
Wilson, S. M. and M. L. Serre (2007), Examination of atmospheric ammonia levels near hog CAFOs, homes and schools in Eastern North Carolina, *Atmos. Environ., 41,* 4977-4987.

Table 1. Measurement techniques for gaseous species, planetary boundary layer (PBL) dynamics, and meteorological parameters.

Species/parameter	Measurement technique
NH_3	Daylight Solutions External Cavity Quantum Cascade Laser (Photo-acoustic Spectroscopy)
CO	Thermo Electron Corp. 48C Trace Level CO Analyzer (Gas Filter Correlation)
SO_2	Thermo Electron Corp. 43C Trace Level SO_2 Analyzer (Pulsed Fluorescence)
NO_x	Thermo Electron Corp. 42C Trace Level NO-NO_2-NO_X Analyzer (Chemiluminescence)
NO_y	Thermo Electron Corp. 42C-Y NO_Y Analyzer (Molybdenum Converter)
HNO_3	Mist Chamber coupled to Ion Chromatography (Dionex, Model CD20-1)
HCl	Mist Chamber coupled to Ion Chromatography (Dionex, Model CD20-1)
VOCs	IONICON Analytik Proton Transfer Reaction Mass Spectrometer and TCEQ Automated Gas Chromatograph
PBL height	Vaisala Ceilometer CL31 with updated firmware to work with Vaisala Boundary Layer View software
Temperature	Campbell Scientific HMP45C Platinum Resistance Thermometer
Wind speed	Campbell Scientific 05103 R. M. Young Wind Monitor
Wind direction	Campbell Scientific 05103 R. M. Young Wind Monitor

Table 2. Statistics of gaseous species data collected during the measurement period.

	NH_3 (ppb)	CO (ppb)	NO_x (ppb)	NO_y (ppb)	SO_2 (ppb)	HNO_3 (ppt)	HCl (ppt)
Mean	2.68	137.12	3.52	5.84	0.42	533.24	350.53
Standard Deviation	1.59	42.43	4.21	4.61	0.52	519.02	277.12
Maximum	10.07	359.71	28.53	31.62	6.82	5039.31	1883.61
Minimum	0.35	75.94	0.51	1.12	0.01	44.55	23.84
Median	2.33	127.55	1.92	4.33	0.35	376.82	283.86
10th Percentile	0.35	93.82	0.71	2.34	0.12	125.26	92.45
25th Percentile	1.53	106.23	1.02	3.08	0.23	210.47	153.06
75th Percentile	3.62	153.14	4.34	6.75	0.42	648.62	470.87
90th Percentile	5.13	197.92	8.55	11.36	0.83	1104.34	676.59

Table 3. Pearson's correlation coefficients (r) between NH_3 and other air pollutants during different measurement periods.

	Weekday	Saturday	Sunday	Daytime	Nighttime
NH_3 vs. CO	0.09	0.11	0.62	0.31	0.41
NH_3 vs. NO_x	0.11	0.09	0.43	0.11	0.26
NH_3 vs. NO_y	0.09	0.08	0.57	0.21	0.26
NH_3 vs. NO_z	0.03	0.13	0.63	0.09	0.11
NH_3 vs. SO_2	0.06	0.03	0.20	0.12	0.10
NH_3 vs. HNO_3	0.06	0.12	0.67	0.11	0.12
NH_3 vs. HCl	0.46	0.36	0.21	0.18	0.08

List of figures

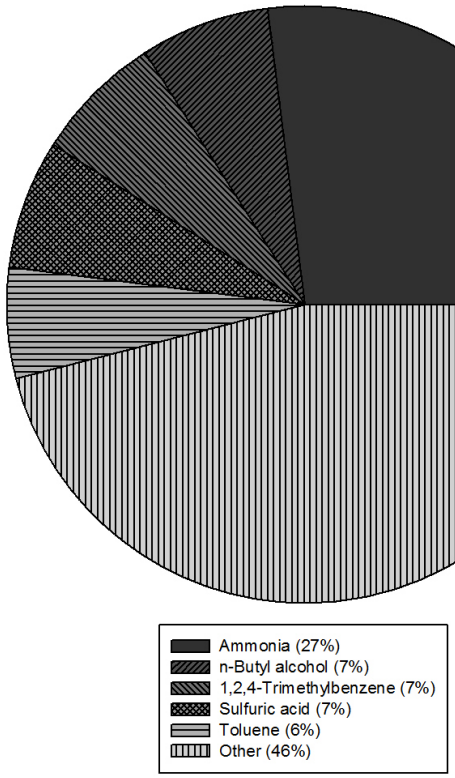
Ammonia (27%)
n-Butyl alcohol (7%)
1,2,4-Trimethylbenzene (7%)
Sulfuric acid (7%)
Toluene (6%)
Other (46%)

(a)

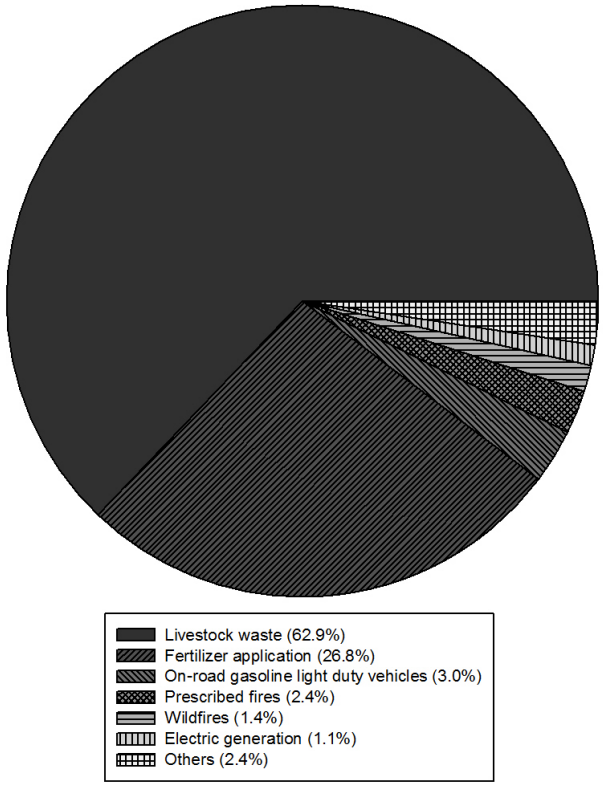
Livestock waste (62.9%)
Fertilizer application (26.8%)
On-road gasoline light duty vehicles (3.0%)
Prescribed fires (2.4%)
Wildfires (1.4%)
Electric generation (1.1%)
Others (2.4%)

(b)

Figure 1.

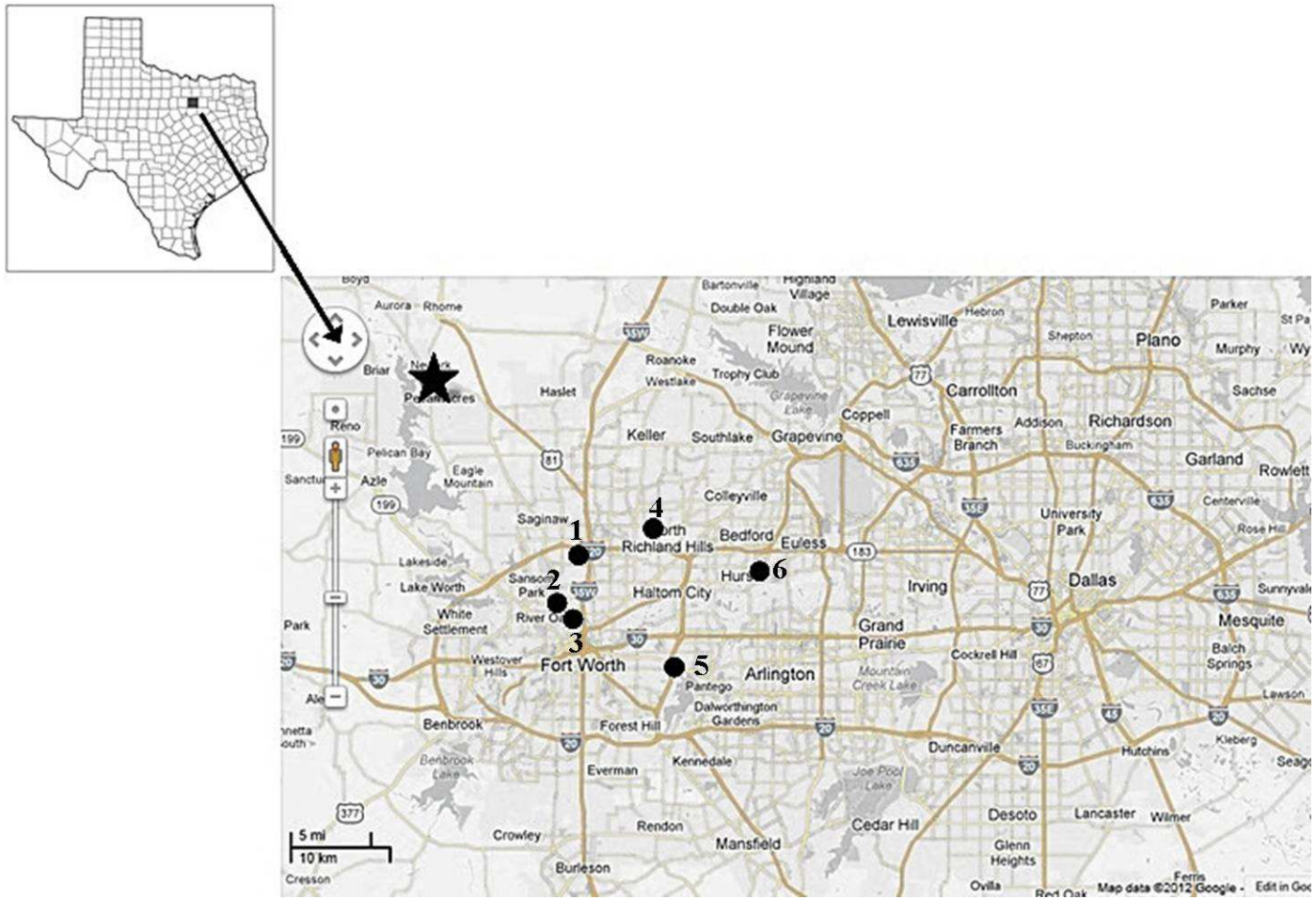
1
2
3
4
5
6
Fort Worth
Arlington
Grand Prairie
Mansfield
Richland Hills
Haltom City
Bedford
Euless
Irving
Dallas
Plano
Carrollton
Lewisville
Flower Mound
Keller
Southlake
Grapevine
Colleyville
Saginaw
Benbrook
Forest Hill
Everman
Kennedale
Duncanville
Cedar Hill
DeSoto
Lancaster
Burleson
Crowley
Rendon
Azle
Haslet
Roanoke
Westlake
Trophy Club
Coppell
Farmers Branch
Addison
Richardson
Garland
Mesquite
University Park
Lake Worth
White Settlement
Westover Hills
Pantego
Dalworthington Gardens
Cockrell Hill
Glenn Heights
Ovilla
5 mi
10 km
Map data ©2012 Google -

Figure 2.

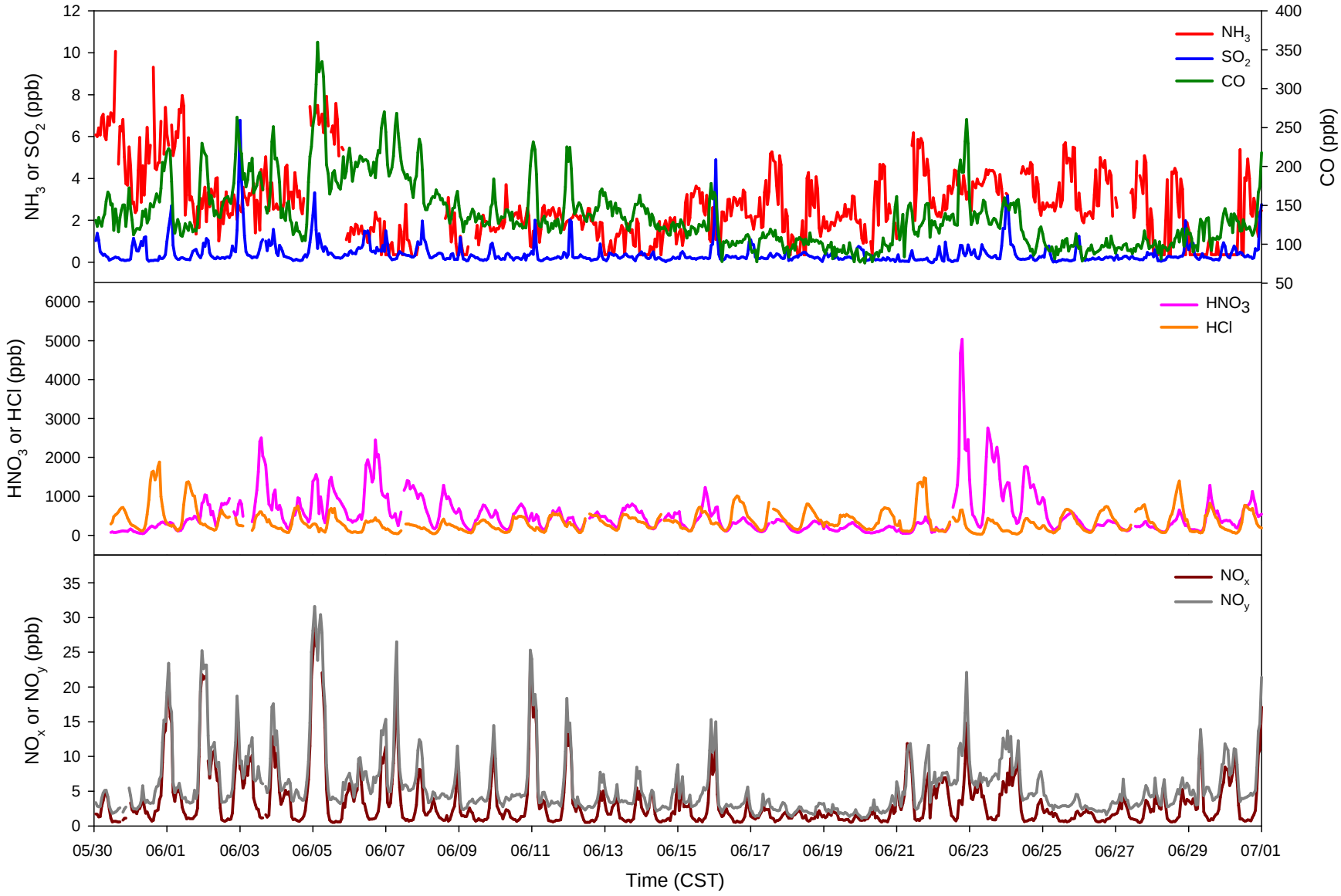
NH3
SO2
CO
NH3 or SO2 (ppb)
CO (ppb)
HNO3
HCl
HNO3 or HCl (ppb)
NOx
NOy
NOx or NOy (ppb)
05/30
06/01
06/03
06/05
06/07
06/09
06/11
06/13
06/15
06/17
06/19
06/21
06/23
06/25
06/27
06/29
07/01
Time (CST)

Figure 3.

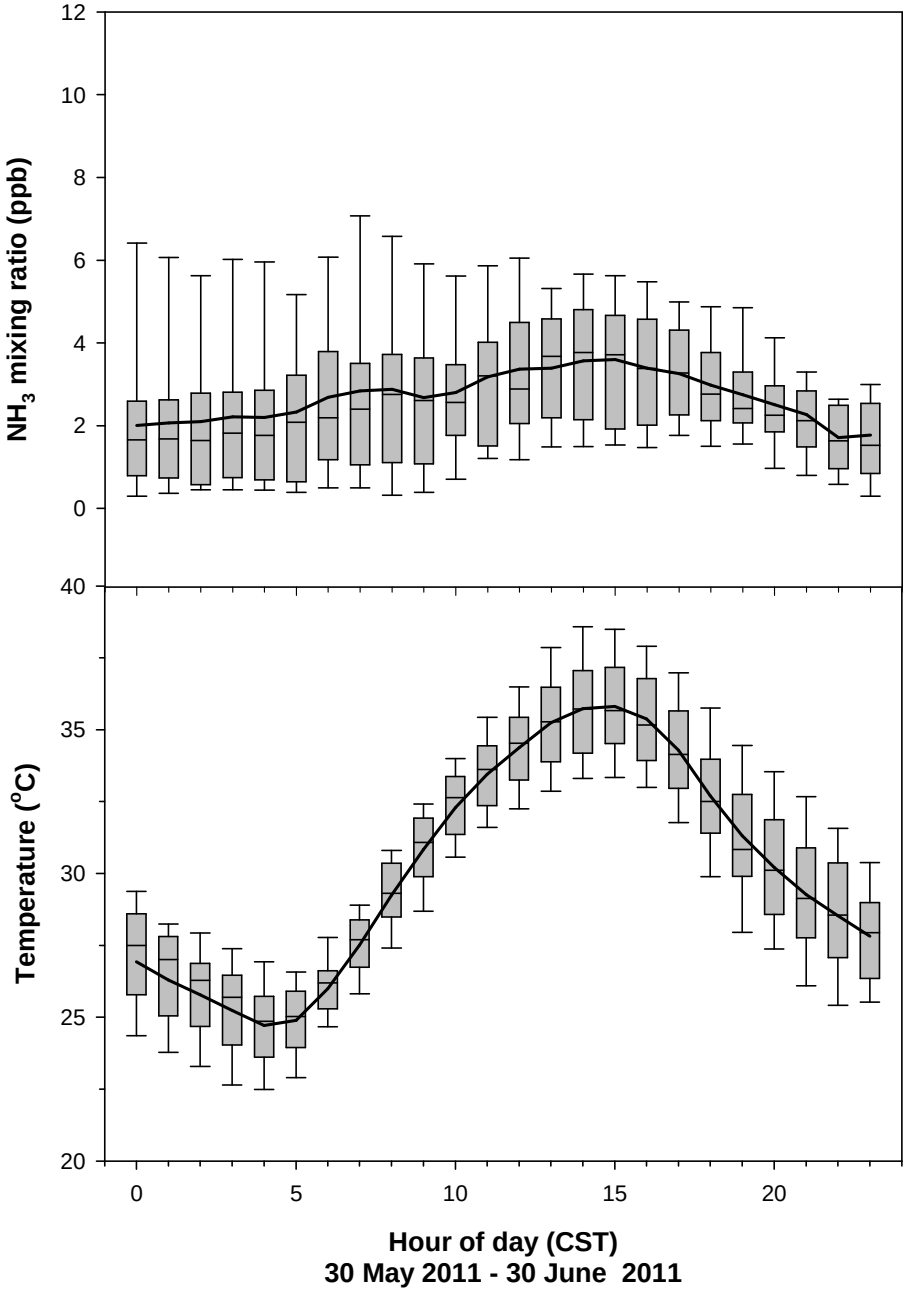
12
10
8
6
4
2
0
NH3 mixing ratio (ppb)
40
35
30
25
20
Temperature (°C)
0
5
10
15
20
Hour of day (CST)
30 May 2011 - 30 June 2011

Figure 4.

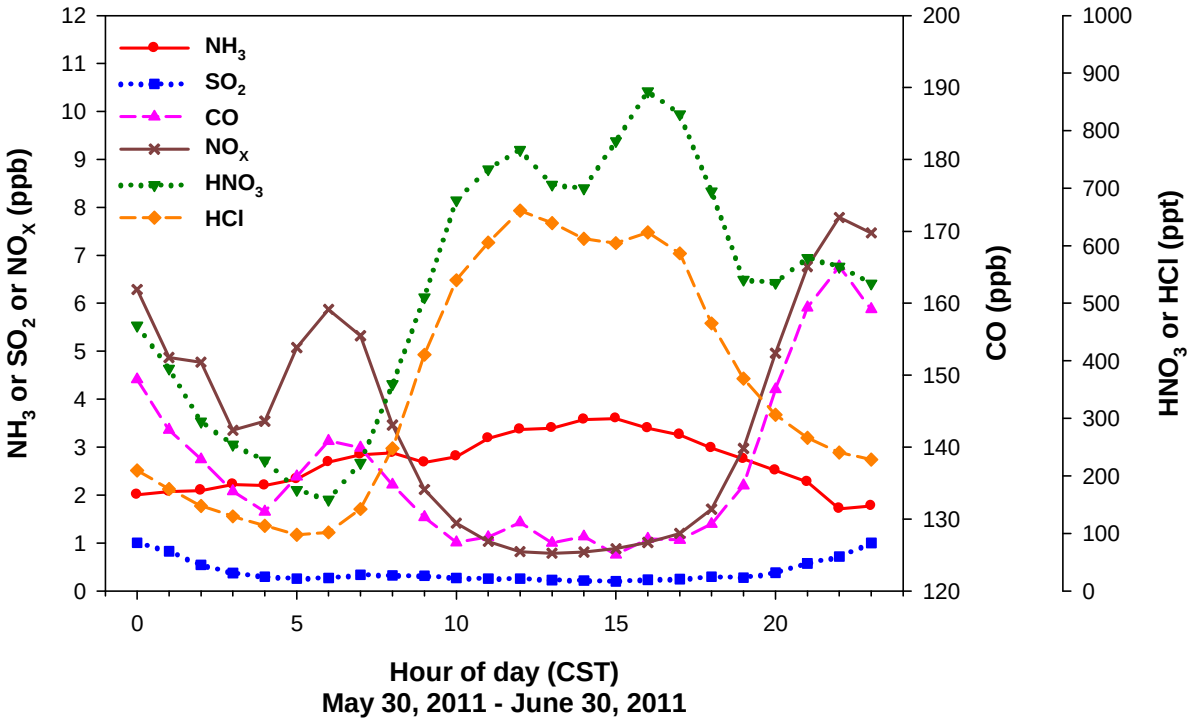
NH3
SO2
CO
NOX
HNO3
HCl
NH3 or SO2 or NOX (ppb)
CO (ppb)
HNO3 or HCl (ppt)
Hour of day (CST)
May 30, 2011 - June 30, 2011

Figure 5.

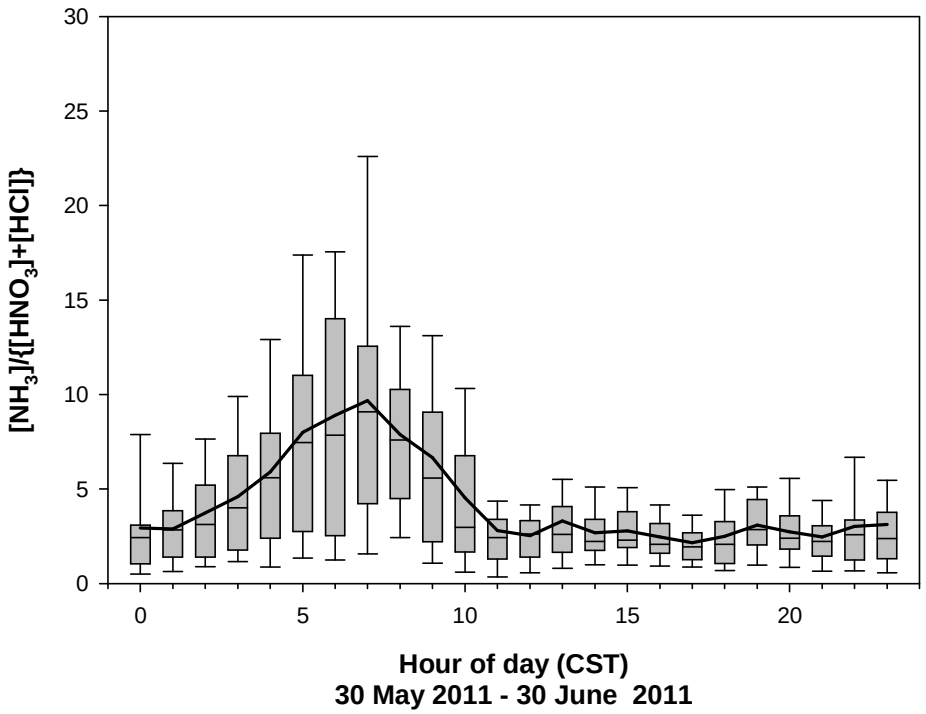
30
25
20
15
10
5
0
0
5
10
15
20
[NH3]/{[HNO3]+[HCl]}
Hour of day (CST)
30 May 2011 - 30 June 2011

Figure 6.

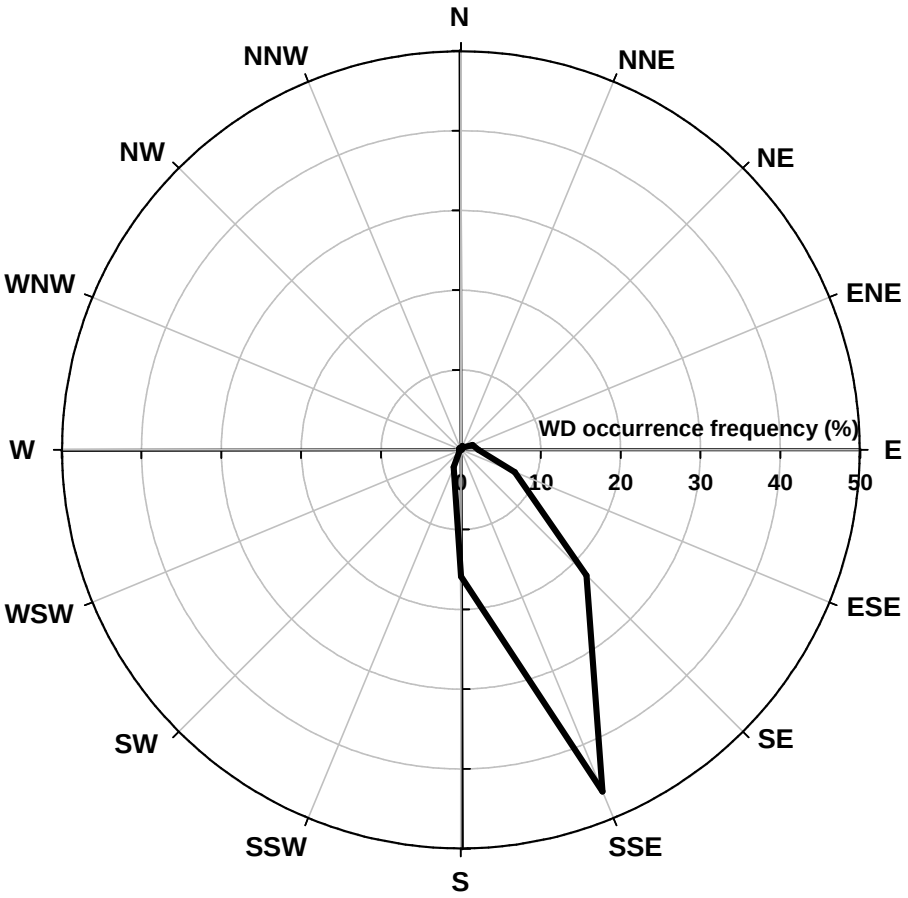

May 30, 2011 - June 30, 2011

Figure 7.